Article

Biodegradable Nanofiber for Delivery of Immunomodulating Agent in the Treatment of Basal Cell Carcinoma

Richard Garrett [1,2], Eri Niiyama [2,3], Yohei Kotsuchibashi [2], Koichiro Uto [2] and Mitsuhiro Ebara [2,4],*

[1] Department of Chemistry and Physics, La Trobe University, Bundoora, Victoria 3086, Australia;
E-Mail: rggarrett@bigpond.com

[2] International Center for Materials Nanoarchitectonics (WPI-MANA), National Institute for
Materials Science (NIMS), Tsukuba 305-0044, Japan; E-Mails: niyama.eri@nims.go.jp (E.N.);
kotsuchibashi.yohei@nims.go.jp (Y.K.); flatronl1753s@gmail.com (K.U.)

[3] Graduate School of Pure and Applied Sciences, University of Tsukuba, Tsukuba 305-8571, Japan

[4] Department of Material Science and Technology, Graduate School of Tokyo, University of Science,
Tokyo 278-8510, Japan

* Author to whom correspondence should be addressed; E-Mail: ebara.mitsuhiro@nims.go.jp;
Tel.: +81-29-860-4775 or +81-29-860-4708.

Academic Editor: Jinlian Hu

Abstract: In this paper we investigate a potential new treatment option for basal cell carcinoma using electrospun polymer nanofibers. Poly(ε-caprolactone) fibers incorporated with the anti-cancer drug imiquimod were successfully produced for the first time. These fibers were characterized and their diffusion release profile tested *in vitro*. A range of different electrospinning parameters were investigated in order to determine the most effective approach in optimizing the fibers for future *in vivo* testing. Characterization showed stable and homogeneous distribution of imiquimod. Although the drug was released faster than what would be needed to replicate the current treatment model, this system would ideally allow for a treatment option which reduces side effects and is more convenient for the patient than the current topical treatment.

1. Introduction

Skin cancer is the highest incidence cancer across many countries in the world [1–5]. Whilst melanomas have the highest mortality for skin cancers, it is the non-melanoma skin cancers (NMSCs) such as basal cell carcinoma (BCCs) and squamous cell carcinoma (SCCs) that are more common [5]. The economic impact of skin cancers is on the rise so therefore it is necessary to investigate effective but also low cost treatments [6,7]. The current treatment options of NMSCs are extremely varied and very situational [6,8]. Surgical removal of BCCs is favored due to the speed of treatment, particularly for larger tumors [6]. However, an area of healthy skin around the tumor must also be removed to ensure complete excision [9,10]. The exact size of this added margin can vary greatly between surgeons and can be as large as 15 mm [6,9–11]. Factors like location (face, neck, *etc.*) can impose limitations on surgery so other avenues must be sought. The desire to reduce scarring in visible areas alongside the added difficulty of the surgery plays an important role in this decision.

Topical treatments [8] are the most common non-surgical method but other options like radiotherapy [12], photodynamic therapy [13] and cryotherapy [14] have their niches. Combinations of surgical and non-surgical treatment options are also used [8,14]. Imiquimod is one such drugs used as a topical treatment. It is an imidazo-quinoline amine and acts as an immunomodulating agent [15–17]. It is known to induce a range of cytokines and chemokines, in particular, interferon-α (IFN-α) through activation of the Toll-like Receptor 7 (TLR-7) pathway [15–18]. Imiquimod, commonly marketed as Aldara™, is used as a self-administered 5% topical cream for treatment of BCC. Various dosages and treatment periods have been shown to be effective [19–21]. In particular, Geisse *et al.* [21] have showed clearance rates of 75% and 73% over a 6 week period for 5 applications per week and 7 applications per week respectively. The current FDA approved dose of imiquimod in the treatment of BCC is 5 applications per week for 6 weeks [17,22]. However, a common side effect of the treatment is inflammation of the skin at the treatment site as well as scabbing and flaking. In separate randomized, double blind trials by Beutner *et al.* [20] and Geisse *et al.* [21] almost all patients exhibited some form of adverse reaction at the local site of treatment. The severity and frequency of the reactions were seen to increase as the frequency of application was increased. In some cases the reaction was severe enough to require a rest day from treatment. In addition to inflammation, patient compliance [21], difficulty reaching the treatment area (e.g. BCC located on the back) and also the low penetration of the drug into the skin [23] are major problems. Current topical treatments need to have high doses of cancer treating medication to combat poor retention, which can lead to issues of over medication. This also results in a higher cost of treatment.

A possible alternative is to develop a nanotechnology based system for delivery of the anticancer drug into the tumor [24–31]. External patches [32] have been investigated for use with imiquimod [33], however an implantable system has not yet been developed. Poly(ε-caprolactone) (PCL) is an FDA approved biodegradable polymer used for a wide range of biomaterial applications [24,27,34–36]. Moreover, it is easily electrospun into nanofiber using a range of solvents and preparation parameters [34–40]. Electrospinning has a wide range of uses due to the customization available. Fibers can be produced with different length, thickness, tensile strength and many more unique properties. The produced fibers can be on the nanoscale but due to the spin process they are able to form a strong mesh as a macrosystem [35,38,39]. Nanofibers provide excellent applications in biomaterials due to many

properties including high surface area and porosity [36,41–44]. In this work, we look at the viability of a PCL electrospun nanofiber system loaded with imiquimod as a treatment option for basal cell carcinoma by implantation under the tumor. The fiber system could potentially be implanted through a simple procedure like injection or a small incision. Developing this type of system could potentially allow for a great reduction in the dosage required when compared to topical treatments by removing the losses experience through the skin (Figure 1). The high surface area of a nanofiber system would also allow for a fast release of imiquimod from the implant and potentially reduce dosage requirements.
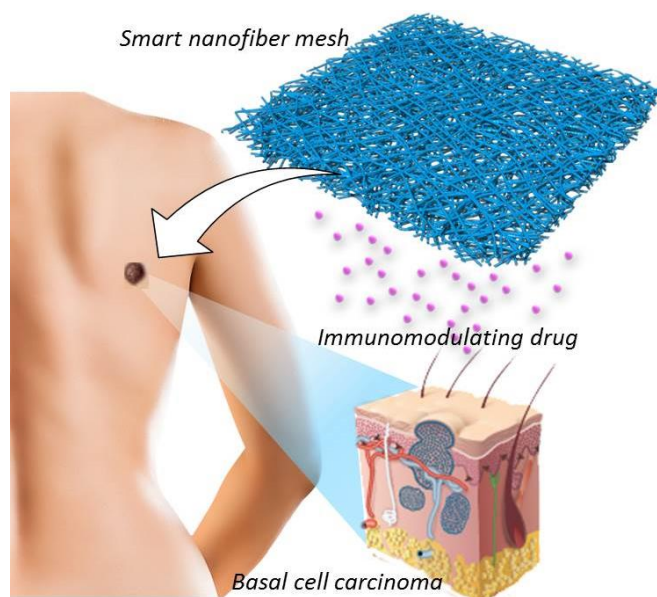

Figure 1. Schematic illustration for the nanofiber-based treatment of basal cell carcinoma.

2. Experimental Section

2.1. Preparation of Poly(ε-caprolactone) (PCL)

PCL were synthesized by ring-opening polymerization from terminal hydroxyl groups of tetrametylene glycol using tin octoate as a catalyst [45,46]. The ε-caprolactone (105 mL, 0.99 mol) and 1,4-butandiol (221 μL, 2.47 mmol) were placed in round-bottom flask under N_2 gas. Tin(II) 2-ethylhexanoate (0.50 mmol) was dropped into the reaction flask. The mixing solution was allowed to react under stirring at 120 ℃ for 72 h. The product was completely dissolved in tetrahydrofuran (THF). The obtained PCL was purified by reprecipitation from hexane and diethylether. ^{1}H NMR (300 MHz, CDCl$_3$): δ/ppm 1.3 (m, 2H, C*H*$_2$ backbone), 1.6 (m, 4H, C*H*$_2$ backbone), 2.2 (m, 2H, C*H*$_2$ backbone), 3.6 (t, –C*H*$_2$OH end group), 4.0 (m, 2H, OC*H*$_2$ backbone).

2.2. Fiber Production

Nanofibers were produced through electrospinning the PCL using an applied voltage of 20 kV (Nanon-01A, MECC Co., Ltd., Fukuoka, Japan) with an 11 cm needle and collector plate separation. The flow rate and PCL to solvent (hexafluoro-2-propanol (HFIP)) ratio (w/v%) were varied in order to produce different fibers. Each set of parameters were used for a 5 wt% and 10 wt% loading of imiquimod.

2.3. Characterization

Fiber morphology was characterized using a FE-SEM (SU8000, Hitachi High-Technologies Corporation, Tokyo, Japan) at 1 kV. Samples were coated with ~3 nm of platinum before imaging due to the poor reflectivity of the PCL. Images were analyzed using ImageJ software. Energy Dispersive X-Ray Spectroscopy (FE-SEM SU8000 EDX, Hitachi High-Technologies Corporation, Tokyo, Japan) Mapping (with Bruker QUANTAX EDS for SEM, 5 kV) for the Nitrogen in the imiquimod was used to show the localization of the drug within the fibers. ^{1}H NMR (300 MHz JNM AL300, JEOL Ltd., Tokyo, Japan) was used to investigate the molecular weight and molecular ratio of PCL to imiquimod. This produced an approximation of the drug loading within small sections of the fiber. Samples from each mesh (5–10 mg) were solubilized in $CDCl_3$ with HFIP (96:4). The molecular weight (M_n) and polydispersity (M_w/M_n) of PCL were determined by gel permeation chromatography (GPC) with columns of TOSOH TSK-GEL α-2500 and α-4000 (Tosoh, Tokyo, Japan) and a RI-2031 refractive index detector (JASCO International Co., Ltd., Tokyo, Japan) (THF, 30 °C, 1.0 mL/min). XRD (Rint 2000 Ultima- III, RIGAKU Corporation, Tokyo, Japan) was used for X-ray Diffraction analysis of the fibers. Samples were scanned from 5 ° to 45 ° at a scan rate of 1 °/min. Scanning occurred at 40 kV/40 mA using a Cu target Kα source.

2.4. Drug Release Profile

1.5 cm^2 segments of each fiber mesh (performed in triplicate) were weighed and placed in individual tubes. 100 mL of pre-warmed Phosphate Buffered Saline (PBS, pH 7.4, Sigma-Aldrich, Tokyo, Japan) was added to each tube and placed into 37 °C shaking water bath in order to mimic the conditions seen in the body. As the electrospinning process creates layers of polymer in an arbitrary manner the resulting mesh is often not uniform with areas of the same mesh exhibiting different fiber distributions. The segments were cut to 1.5 cm^2 sections in order to eliminate variance in the drug release due to the size and shape of the sample. The segments varied in weight between 0.73 mg and 3.82 mg. At specified time intervals, 2 mL of solution was removed from each tube and replaced with fresh, pre-warmed PBS in order to maintain the total volume through the trial. The removed solutions were analyzed for imiquimod concentration with UV-Vis spectroscopy using a Jasco V-650 spectrophotometer.

3. Results and Discussion

3.1. SEM of PCL/Imiquimod Nanofibers

The molecular weight and polydispersity of PCL were summarized in Table 1. The calculated molecular weights agreed between ^{1}H NMR ($M_{n,NMR}$ = 27,600 g/mol) and GPC ($M_{n,GPC}$ = 27,000 g/mol) results and the polydispersity was relatively narrow (M_w/M_n = 1.35).

Table 1. Characteristic data of poly(ε-caprolactone) (PCL).

PCL	$M_{n,NMR}$ (g/mol)	$M_{n,GPC}$ (g/mol)	M_w/M_n (-)
	27,600	27,000	1.35

The characterization of PCL/Imiquimod fibers was shown in Table 2. The prepared fibers with no drug were considerably larger than their drug-inclusive counterparts. The fiber size showed no consistent trend between differing imiquimod concentrations. Figure 2 shows only slight differences in the surfaces of the fibers. In particular, the 10 wt% fibers (sample B) showed small nodules on the surface more frequently than the 5 wt% fibers (sample A). EDX mapping of Nitrogen in the fibers can be seen in Figure 3 showing that there is no nucleation of imiquimod within the fibers due to the even distribution of the Nitrogen signal shown as green dots. This was consistent across all samples. A non-homogeneous distribution would create issues in the practicality of this type of system as the local concentration may not be representative of the entire system. Any aggregation of the imiquimod could alter the release of the drug from the system due to the changes to the particle size.
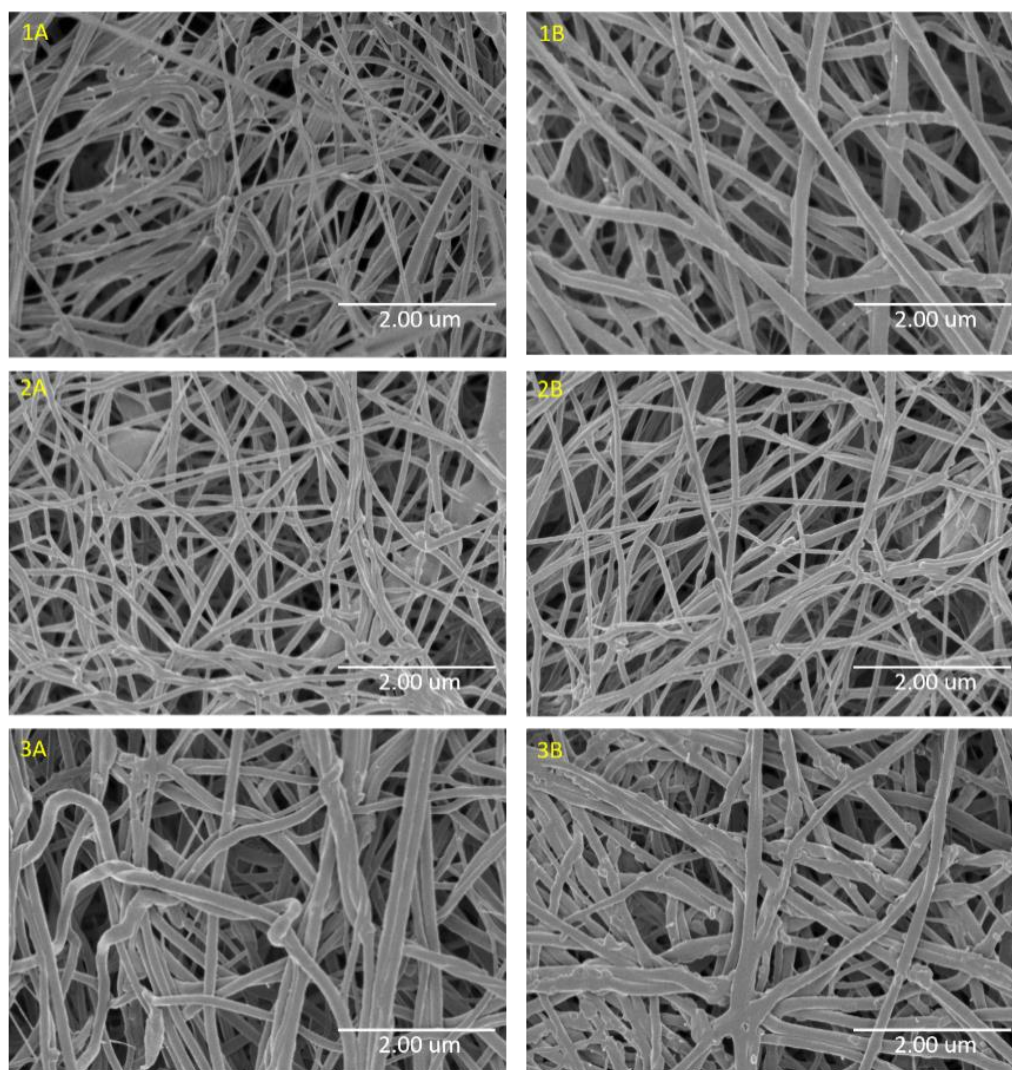

Figure 2. 1 kV SEM images of each PCL/imiquimod nanofiber sample. The images are labeled with the sample name shown in Table 2.

Table 2. Electrospinning variables and fiber size analysis of PCL/Imiquimod nanofibers.

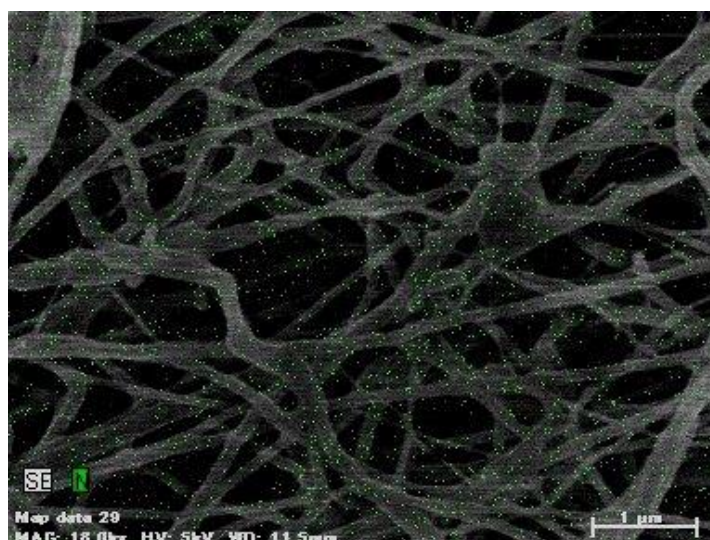| Sample	PCL w/v%	Flow rate (mL/h)	Imiquimod wt%	Average fiber size (nm) ±standard deviation
1	15	1	0	540 ±281
1A	15	1	5	72 ±22
1B	15	1	10	120 ±56
2	15	2	0	1028 ±382
2A	15	2	5	94 ±20
2B	15	2	10	95 ±92
3	20	1	0	1320 ±504
3A	20	1	5	132 ±33
3B	20	1	10	150 ±36

Figure 3. Energy Dispersive X-Ray Spectroscopy (EDX) mapping of sample 1A showing the nitrogen signal produced by imiquimod (green). Signal was detected for 1 min 30 s. Homogeneous distribution was seen across all samples.

3.2. X-Ray Diffraction

XRD scan results are shown in Figure 4. The imiquimod only sample (A) shows clear peaks due to the crystalline nature of the imiquimod powder. These peaks are not seen in the fiber samples which confirms that imiquimod is not in a crystalline state. Crystallization would increase the particle size significantly which would also interfere with the release of imiquimod. The results of the XRD and EDX mapping suggest that the electrospinning process allows for a homogeneous distribution of imiquimod inside of the nanofibers with no crystallization occurring.
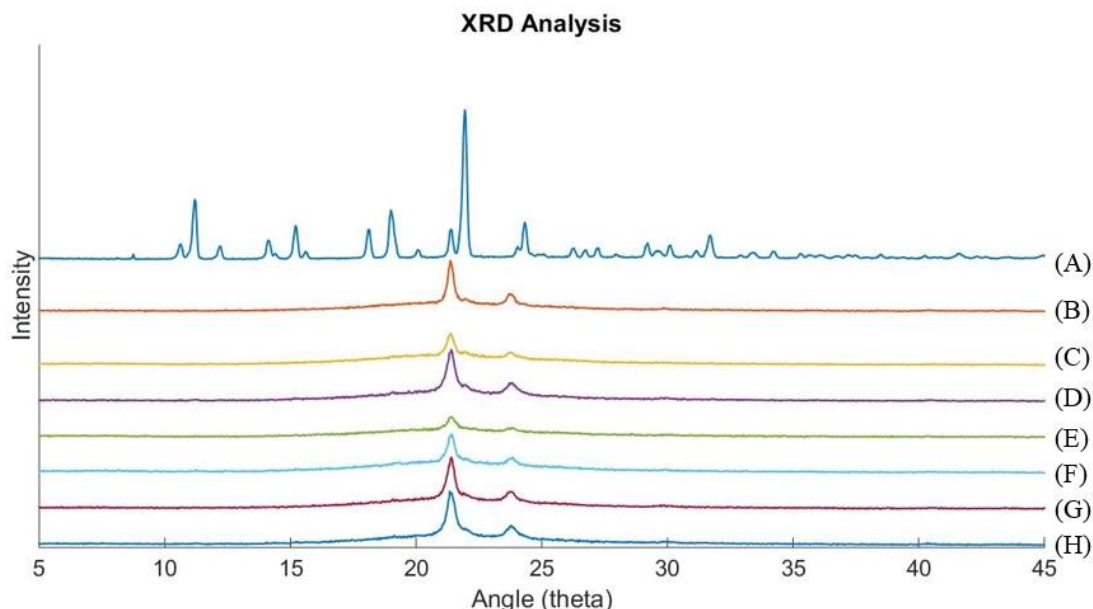
Figure 4. XRD results for imiquimod only (**A**), PCL only (**B**) and samples 1A, 1B, 2A, 2B, 3A, 3B (C to H respectively). The fiber samples only exhibit peaks for PCL and do not show any indication of imiquimod crystallinity due to no peaks observed matching the imiquimod only sample.

3.3. Drug Release Profile

First, the content of imiquimod in the nanofiber was measured using ^{1}H NMR (^{1}H NMR, CDCL$_3$/HFIP (96:4), 25 °C: δ (ppm) 7.93 (d, 1H), 7.83 (d, 1H), 7.79 (s, 1H), 7.58 (t, 1H), 7.40 (t, 1H)). Peaks seen for PCL were as reported in Sinnwell, *et al.* [47]. From analysis of the molecular ratio between PCL and imiquimod peaks, the wt% of imiquimod was seen to be at the intended concentration (~±1 wt%). This measurement confirms that the signals detected in earlier EDX measurements were produced by imiquimod whilst also showing that imiquimod was still within an acceptable range of the intended concentration.

Imiquimod release from the fibers in PBS was initially noted to max at ~4 µg/mL. Therefore the total volume (100 mL) was chosen to guarantee that even with 100% drug release, the total concentration would remain below this limit. Drug release rate is extremely important for this type of system as the drug needs to maintain an effective concentration at the treatment site for an appropriate duration. Failing to do so could cause potential underdosing and subsequent failure to treat the problem.

Figure 5 shows that all imiquimod was released in varying time periods over 48 h. The rate of release was averaged for all replicates of each sample. The samples were cut into 1.5 cm^2 square segments in order to maintain consistency for size and shape. Due to the non-uniform distribution of fibers produced by electrospinning, the thicknesses of each segment varied at different locations in the mesh. Therefore the samples were weighed in order to determine the total amount of imiquimod within the fiber. The heavier segments were subsequently accepted as being thicker than the lighter segments due to each sample being the same area. The total amount of imiquimod within the sample was taken as 5% (Sample a) or 10% (Sample B) of the total weight but as there was a variance of ±~1 wt% some samples showed greater than 100% release implying these samples had more than the 5 wt% or 10 wt% of imiquimod.

Figure 6A shows there is an apparent trend in which the weight of the sample affects the release rate likely due to the smaller surface area to volume ratio (SA:V) seen for thicker samples. During the release tests, the fibers initially were an opaque white. However, as the release progressed, the fibers became slightly transparent. The heavier samples (smaller SA:V ratio) took a longer time to reach this transparent state. It was noted that at this time point, the release rate of the drug greatly increased. It was believed that this is the transparency occurred by the "wetting" of the fibers. Imiquimod is a very small molecule which increases its potential for rapid diffusion. Therefore, it is possible that the imiquimod releases as soon as the PBS "wets" the sample area. The smaller the SA:V ratio for the fiber mesh, the longer it takes for the PBS to penetrate. In order to investigate this hypothesis, the electrospinning conditions used for Sample 3A were repeated but with 3 times the volume. This created a much thicker mesh sample (labeled 3A-Thick). Parameters for sample 3 were chosen due to the fibers produced being more stable and easier to handle than the other options. Drug release testing was repeated with a 1.5 cm^2 3A-Thick sample. The 3A-Thick tests showed the same trend for drug release as seen earlier. The thicker 3A-Thick samples were slower to release and also due to the added thickness, contained a larger dosage of drug (Figure 6B).
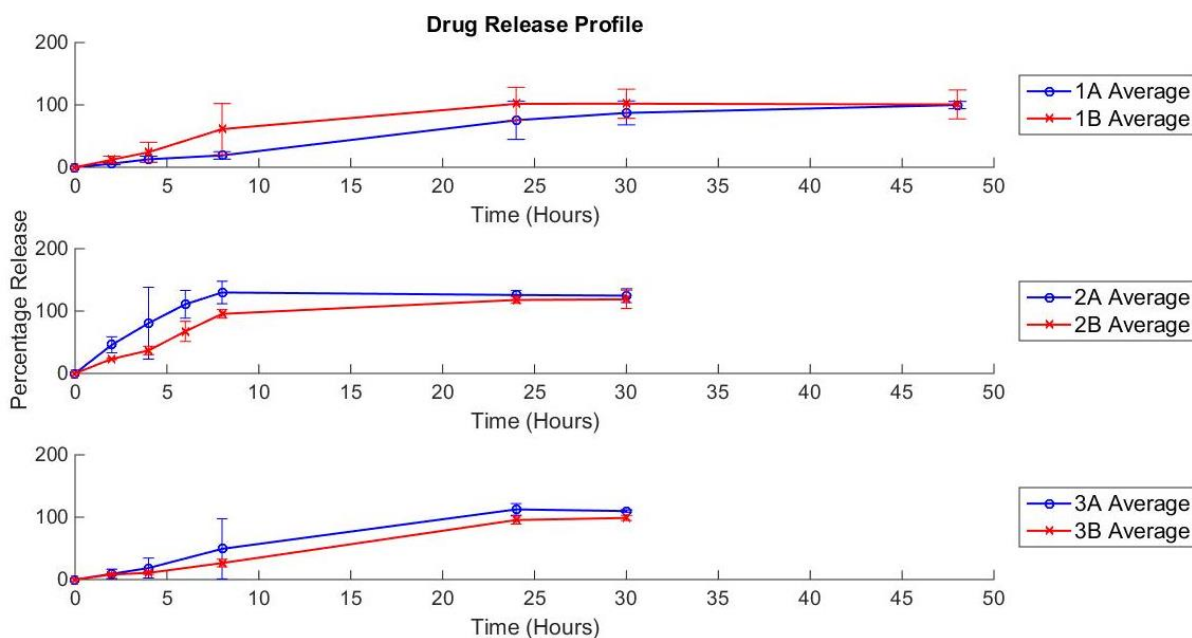

Figure 5. Drug release profiles for all samples. The profile shown is the average for all 3 technical replicates. 100% drug release assumed 5 wt% and 10 wt% (sample A and B respectively) loading of imiquimod.
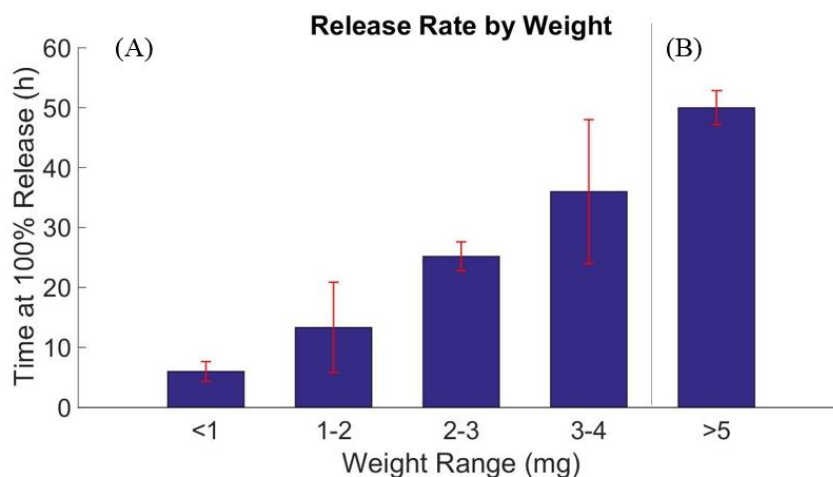
Figure 6. (**A**) Release rate *vs.* weight for original samples. The release rate time was determined by the first measurement where the drug concentration no longer increased. $n = 3$, 6, 5 and 4 from left to right; (**B**) Additional test showing results for sample 3A-Thick for comparison the original lighter samples. $n = 3$.

It is important to find a balance between what is an effective treatment dosage and the release duration. Miller *et al.* [48] showed the effective concentration of imiquimod in human cells to initiate a response was between 1 and 5 μg/mL. Fibers could be customized to maintain this effective concentration with an adequate release rate. However, release rates presented in this paper would likely be much faster than desired for an *in vivo* model. Current estimates for an effective drug delivery system would match closely with the current ~6 week treatment period used for the topical cream. In order to achieve a slower release there has been great promise in a range of techniques. The use of dendrimers [49], PEG conjugates [50,51] or micelles [52,53] are all viable options for slowing the release of drugs. These types of systems could either make the imiquimod part of a bigger molecule or trap the imiquimod into a multi-stage release. However, to be a feasible treatment this system must not inhibit the mechanism of action for imiquimod. Therefore whilst further investigation is necessary into the compatibility of imiquimod with these types of release mechanisms it is promising that a suitable option can be found.

4. Conclusions

Electrospinning provides a wide range of parameters for customizing PCL nanofibers. In combination with the anti-cancer drug imiquimod, fibers were produced with homogeneous distribution of the drug. The created fiber samples showed excellent potential for a diffusion release system. However the rate of release was faster than optimal. By combining this technology with drug encapsulation methods, a viable solution for a slower release rate can be found. With optimal customization of the release rate and the total dosage within the fibers, this system may be used for drug delivery to basal cell carcinomas. This could allow for a treatment option which reduces side effects significantly and is more convenient for the patient than the current topical treatment.

Acknowledgments

Author Contributions

Fiber design and fabrication was performed by Richard Garrett, Eri Niiyama and Koichiro Uto. Fiber characterisation was performed by Richard Garrett. Drug release test was designed by Yohei Kotsuchibashi and performed by Richard Garrett. Paper was written by Richard Garrett and Mitsuhiro Ebara.

Conflicts of Interest

The authors declare no conflict of interest.

References

1. Staples, M.P.; Elwood, M.; Burton, R.C.; Williams, J.L.; Marks, R.; Giles, G.G. Non-melanoma skin cancer in australia: The 2002 national survey and trends since 1985. *Med. J. Aust.* **2006**, *184*, 6–10.
2. Katalinic, A.; Kunze, U.; Schäfer, T. Epidemiology of cutaneous melanoma and non-melanoma skin cancer in schleswig-holstein, germany: Incidence, clinical subtypes, tumour stages and localization (epidemiology of skin cancer). *Br. J. Dermatol.* **2003**, *149*, 1200–1206.
3. Hoey, S.E.H.; Devereux, C.E.J.; Murray, L.; Catney, D.; Gavin, A.; Kumar, S.; Donnelly, D.; Dolan, O.M. Skin cancer trends in northern ireland and consequences for provision of dermatology services. *Br. J. Dermatol.* **2007**, *156*, 1301–1307.
4. Jung, G.W.; Metelitsa, A.I.; Dover, D.C.; Salopek, T.G. Trends in incidence of nonmelanoma skin cancers in alberta, canada, 1988–2007. *Br. J. Dermatol.* **2010**, *163*, 146–154.
5. Cancer Council Australia. Skin Cancer. Available online: http://www.cancer.org.au/about-cancer/types-of-cancer/skin-cancer.html (accessed on 1 September 2015).
6. Madan, V.; Lear, J.T.; Szeimies, R.-M. Non-melanoma skin cancer. *Lancet* **2010**, *375*, 673–685.
7. Sinclair, R. Nonmelanoma skin cancer in australia. *Br. J. Dermatol.* **2013**, *168*, 1–2.
8. Bahner, J.D.; Bordeaux, J.S. Non-melanoma skin cancers: Photodynamic therapy, cryotherapy, 5-fluorouracil, imiquimod, diclofenac, or what? Facts and controversies. *Clin. Dermatol.* **2013**, *31*, 792–798.
9. Santiago, F.; Serra, D.; Vieira, R.; Figueiredo, A. Incidence and factors associated with recurrence after incomplete excision of basal cell carcinomas: A study of 90 cases. *J. Eur. Acad. Dermatol. Venereol.* **2010**, *24*, 1421–1424.
10. Wolf, D.J.; Zitelli, J.A. Surgical margins for basal cell carcinoma. *Arch. Dermatol.* **1987**, *123*, 340–344.

11. Smeets, N.W.J.; Kuijpers, D.I.M.; Nelemans, P.; Ostertag, J.U.; Verhaegh, M.E.J.M.; Krekels, G.A.M.; Neumann, H.A.M. Mohs' micrographic surgery for treatment of basal cell carcinoma of the face—Results of a retrospective study and review of the literature. *Br. J. Dermatol.* **2004**, *151*, 141–147.

12. Barnes, E.A.; Breen, D.; Culleton, S.; Zhang, L.; Kamra, J.; Tsao, M.; Balogh, J. Palliative radiotherapy for non-melanoma skin cancer. *Clin. Oncol.* **2010**, *22*, 844–849.

13. Hamdoon, Z.; Jerjes, W.; Upile, T.; Hopper, C. Optical coherence tomography-guided photodynamic therapy for skin cancer: Case study. *Photodiagn. Photodyn. Ther.* **2011**, *8*, 49–52.

14. Kokoszka, A.; Scheinfeld, N. Evidence-based review of the use of cryosurgery intreatment of basal cell carcinoma. *Dermatol. Surg.* **2003**, *29*, 566–571.

15. Sauder, D.N. Imiquimod: Modes of action. *Br. J. Dermatol.* **2003**, *149*, 5–8.

16. Stanley, M.A. Imiquimod and the imidazoquinolones: Mechanism of action and therapeutic potential. *Clin. Exp. Dermatol.* **2002**, *27*, 571–577.

17. Chang, Y.C.; Madkan, V.; Cook-Norris, R.; Sra, K.; Tyring, S. Current and potential uses of imiquimod. *South. Med. J.* **2005**, *98*, 914–920.

18. Dahl, M.V. Imiquimod: An immune response modifier. *J. Am. Acad. Dermatol.* **2000**, *43*, 1–5.

19. Turan, A.; Saricaoglu, H.; Baskan, E.B.; Toker, S.C.; Tunali, S. Treatment of infiltrating basal cell carcinoma with the combination of intralesional ifnα-2b and topical imiquimod 5% cream. *Int. J. Dermatol.* **2009**, *48*, 215–217.

20. Beutner, K.R.; Geisse, J.K.; Helman, D.; Fox, T.L.; Ginkel, A.; Owens, M.L. Therapeutic response of basal cell carcinoma to the immune response modifier imiquimod 5% cream. *J. Am. Acad. Dermatol.* **1999**, *41*, 1002–1007.

21. Geisse, J.; Caro, I.; Lindholm, J.; Golitz, L.; Stampone, P.; Owens, M. Imiquimod 5% cream for the treatment of superficial basal cell carcinoma: Results from two phase iii, randomized, vehicle-controlled studies. *J. Am. Acad. Dermatol.* **2004**, *50*, 722–733.

22. Food and Drug Administration. *Imiquimod Prescribing Information*; Food and Drug Administration: Silver Spring, MD, USA, 2010.

23. Taveira, S.F.; Lopez, R.F.V. *Topical Administration of Anticancer Drugs for Skin Cancer Treatment*; In *Skin Cancers—Risk, Factors, Prevention and Therapy*; InTech: Rijeka, Croatia, 2011; Chapter 11.

24. Chen, W.; Wu, Z.; Yang, H.; Guo, S.; Li, D.; Cheng, L. *In vitro* and *in vivo* evaluation of injectable implants for intratumoral delivery of 5-fluorouracil. *Pharm. Dev. Technol.* **2014**, *19*, 223–231.

25. Cheng, C.; Wei, H.; Zhang, X.-Z.; Cheng, S.-X.; Zhuo, R.-X. Thermo-triggered and biotinylated biotin-p(nipaam-co-hmaam)-b-pmma micelles for controlled drug release. *J. Biomed. Mater. Res. A* **2009**, *88*, 814–822.

26. Hamidi, M.; Azadi, A.; Rafie, P. Hydrogel nanoparticles in drug delivery. *Adv. Drug Deliv. Rev.* **2008**, *60*, 1638–1649.

27. Hou, J.; Li, C.; Cheng, L.; Guo, S.; Zhang, Y.; Tang, T. Study on hydrophilic 5-fluorouracil release from hydrophobic poly(ε-caprolactone) cylindrical implants. *Drug Dev. Ind. Pharm.* **2011**, *37*, 1068–1075.

28. Ischakov, R.; Adler-Abramovich, L.; Buzhansky, L.; Shekhter, T.; Gazit, E. Peptide-based hydrogel nanoparticles as effective drug delivery agents. *Bioorg. Med. Chem.* **2013**, *21*, 3517–3522.

29. Kim, Y.-J.; Ebara, M.; Aoyagi, T. A smart hyperthermia nanofiber with switchable drug release for inducing cancer apoptosis. *Adv. Funct. Mater.* **2013**, *23*, 5753–5761.

30. Kranz, H.; Bodmeier, R. A novel *in situ* forming drug delivery system for controlled parenteral drug delivery. *Int. J. Pharm.* **2007**, *332*, 107–114.

31. Zeng, R.; Tu, M.; Liu, H.-W.; Zhao, J.-H.; Zha, Z.-G.; Zhou, C.-R. Preparation, structure and drug release behaviour of chitosan-based nanofibre. *IET Nanobiotechnol.* **2009**, *3*, 8–13.

32. Donnelly, R.F.; McCarron, P.A.; Morrow, D.I.J.; Woolfson, A.D. Fast-drying multi-laminate bioadhesive films for transdermal and topical drug delivery. *Drug Dev. Ind. Pharm.* **2013**, *39*, 1818–1831.

33. Donnelly, R.F.; McCarron, P.A.; Zawislak, A.A.; Woolfson, A.D. Design and physicochemical characterisation of a bioadhesive patch for dose-controlled topical delivery of imiquimod. *Int. J. Pharm.* **2006**, *307*, 318–325.

34. Alves da Silva, M.L.; Martins, A.; Gomes, M.; Costa-Pinto, A.R.; Reis, R.L.; Costa, P.; Neves, N.M. Cartilage tissue engineering using electrospun PCL nanofiber meshes and MSCs. *Biomacromolecules* **2010**, *11*, 3228–3236.

35. Huang, Z.-M.; Zhang, Y.-Z.; Kotaki, M.; Ramakrishna, S. A review on polymer nanofibers by electrospinning and their applications in nanocomposites. *Compos. Sci. Technol.* **2003**, *63*, 2223–2253.

36. Namekawa, K.; Schreiber, M.T.; Aoyagi, T.; Ebara, M. Fabrication of zeolite-polymer composite nanofibers for removal of uremic toxins from kidney failure patients. *Biomater. Sci.* **2014**, *2*, 674–679.

37. Bordes, C.; Fréville, V.; Ruffin, E.; Marote, P.; Gauvrit, J.Y.; Briancon, S.; Lantéri, P. Determination of polycaprolactone solubility parameters: Application to solvent substitution in a microencapsulation process. *Int. J. Pharm.* **2010**, *383*, 236–243.

38. Gholipour Kanani, A.; Hajir Bahrami, S. Effect of changing solvents on poly(ε-caprolactone) nanofibrous webs morphology. *J. Nanomater.* **2011**, *2011*, 1–10.

39. Qin, X.; Wu, D. Effect of different solvents on poly(caprolactone) (PCL) electrospun nonwoven membranes. *J. Therm. Anal. Calorim.* **2012**, *107*, 1007–1013.

40. Dias, J.; Bártolo, P. Morphological characteristics of electrospun PCL meshes—The influence of solvent type and concentration. *Procedia CIRP* **2013**, *5*, 216–221.

41. Kim, Y.-J.; Ebara, M.; Aoyagi, T. Temperature-responsive electrospun nanofibers for "on–off" switchable release of dextran. *Sci. Technol. Adv. Mater.* **2012**, *12*, 064203:1–064203:9.

42. Kim, Y.-J.; Ebara, M.; Aoyagi, T. A smart nanofiber web that captures and releases cells. *Angew. Chem. Int. Ed.* **2012**, *51*, 10537–10541.

43. Wang, Y.; Kotsuchibashi, Y.; Uto, K.; Ebara, E.; Aoyagi, T.; Liu, Y.; Narain, R. pH and glucose responsive nanofibers for the reversible capture and release of lectins. *Biomater. Sci.* **2015**, *3*, 152–162.

44. Wang, Y.; Kotsuchibashi, Y.; Liu, Y.; Narain, R. Study of bacterial adhesion on biomimetic temperature responsive glycopolymer surfaces. *ACS Appl. Mater. Interf.* **2015**, *7*, 1652–1661.

45. Ebara, M.; Uto, K.; Idota, N.; Hoffman, J.M.; Aoyagi, T. Shape-memory surface with dynamically tunable nanogeometry activated by body heat. *Adv. Mater.* **2012**, *24*, 273–278.

46. Chmura, A.J.; Davidson, M.G.; Jones, M.D.; Lunn, M.D.; Mahon, M.F.; Johnson, A.F.; Khunkamchoo, P.; Roberts, S.L.; Wong, S.S.F. Group 4 complexes with aminebisphenolate ligands and their application for the ring opening polymerization of cyclic esters. *Macromolecules* **2006**, *39*, 7250–7257.

47. Sinnwell, S.; Inglis, A.J.; Davis, T.P.; Stenzel, M.H.; Barner-Kowollik, C. An atom-efficient conjugation approach to well-defined block copolymers using raft chemistry and hetero diels-alder cycloaddition. *Chem. Commun.* **2008**, 2052–2054.

48. Miller, R.L.; Gerster, J.F.; Owens, M.L.; Slade, H.B.; Tomai, M.A. Imiquimod applied topically a novel immune response modifier and new class of drug. *Int. J. Immunopharmacol.* **1999**, *21*, 1–14.

49. Lee, I.-H.; An, S.; Yu, M.K.; Kwon, H.-K.; Im, S.-H.; Jon, S. Targeted chemoimmunotherapy using drug-loaded aptamer-dendrimer bioconjugates. *J. Control. Release* **2011**, *155*, 435–441.

50. Schiavon, O.; Pasut, G.; Moro, S.; Orsolini, P.; Guiotto, A.; Veronese, F.M. PEG-Ara-C conjugates for controlled release. *Eur. J. Med. Chem.* **2004**, *39*, 123–133.

51. Veeren, A.; Bhaw-Luximon, A. Polymer-drug encapsulation using various PEG- and polypeptide-based block copolymer micelles. *Macromol. Symp.* **2012**, *313*, 59–68.

52. Lee, P.; Zhang, R.; Li, V.; Liu, X.; Sun, R.W.; Che, C.-M.; Wong, K.K. Enhancement of anticancer efficacy using modified lipophilic nanoparticle drug encapsulation. *Int. J. Nanomed.* **2012**, *7*, 731–737.

53. Choi, S.-H.; Youn, D.-Y.; Jo, S.M.; Oh, S.-G.; Kim, I.-D. Micelle-mediated synthesis of single-crystalline β(3c)-sic fibers via emulsion electrospinning. *ACS Appl. Mater. Interf.* **2011**, *3*, 1385–1389.